



Analysis of In-Situ Consolidation of Soil by Vacuum Combined Overburden Precompression Blowing and Filling

Leiyong Yang^{1,2,3}, Zhu Liang^{1,2,3}, Qinghua Zhang^{1,2,3,*}

¹ Guangzhou City Planning Survey Design Institute Co., LTD, Guangzhou 510060, China

² Guangdong Enterprise Key Laboratory for Urban Sensing, Monitoring and Early Warning, Guangzhou, 510060, China

³ Collaborative Innovation Center for Natural Resources Planning and Marine Technology of Guangzhou, Guangzhou, 510060, China

*Corresponding author: 499324556@qq.com

Abstract. Based on the monitoring data from a specific base's vacuum joint loading pre-pressure reinforcement project, this analysis delves into aspects such as surface settlement, layered settlement, pore water pressure, and horizontal displacement. The findings reveal that variations in the foundation soil layers of the blow-fill foundation lead to uneven final settlement; the maximum settlement rate during the vacuum stage reaches 18.2mm/d, significantly higher than in subsequent loading and joint loading stages. Additionally, settlement between 6m below the surface accounts for 71.1% of the total settlement, highlighting the effectiveness of the vacuum joint loading preloading method on shallow soil treatment. Furthermore, while increased load enhances soil effective stress, the pore water pressure at 6m depth decreases by -113kPa, surpassing the maximum negative pressure from the vacuum load, indicating the load's impact on the vacuum action process. Lastly, the outward and inward horizontal displacement ratios resulting from the vacuum combined load pre-pressure method correlate with the load ratio—the higher the load ratio, the greater the displacement ratio, and the shallower the critical depth.

Keywords: vacuum combined loading pre-pressure method; pore water pressure; load ratio; blown-fill foundation

1 Introduction

The vacuum precompression method was first proposed by Professor Kjellman[1] of the Royal Swedish Academy of Geology in 1952. However, the practical application of this method is very limited, mainly due to the inability of materials and techniques to generate and maintain vacuum pressure over a large area for a considerable period of time. In the following decades, scholars around the world extensively explored this method[2-6]. Sivaraman [7] et al. conducted experimental research on the vacuum combined load preloading method in the 1980s. In the 1990s, the vacuum combined load

preloading method began to be used in soft foundation reinforcement projects, and the corresponding theoretical basis and practical technology were constantly improved. Dong Song [8] systematically introduced the ground settlement, consolidation, and seepage calculation theories of the vacuum combined pile preloading method in 2009. Sun [9] believed in 2014 that there was a positive correlation between deep horizontal displacement and vertical settlement of soil mass and that lateral displacement and vertical settlement would promote each other. Zhang [10] explained that the pore water pressure of the vacuum combined preloading method continued to decrease after a sudden increase because the vacuum load was much larger than the pile load, and vacuum preloading always dominated in the combined preloading stage. Some foreign scholars have also analyzed the actual engineering effect of vacuum precompression method [11-15].

The soil foundation is mainly filled with silt, silty clay, and fine sand, which generally has the characteristics of high moisture content, low strength, large pore ratio and high sensitivity. This project analyzes the effect of vacuum combined preloading method on the treatment of the blown fill soil foundation, summarizes the change law of settlement, pore water pressure and stratified settlement during the reinforcement process, explores the reinforcement mechanism of vacuum combined loading reason method, and provides reference for other blown fill soil foundation treatment projects.

2 Project Overview and Geological Conditions

2.1 Project Profile

The project is a foundation-strengthening initiative, divisible into the southern, central, and northern zones from south to north. The southern zone primarily undergoes vacuum combined preloading treatment, with the M-A5 area situated at its center, covering approximately 26,649 square meters. During the reinforcement of the M-A5 area, the vacuum beneath the film remains relatively stable, ensuring the construction process is uninterrupted by external factors. Given the significant research value of field data, this paper delves into the analysis of the M-A5 region.

The entire M-A5 area employs vacuum combined preloading treatment. The construction procedure is as follows: the surface is cleaned and a 0.5-meter thick sand cushion is laid; B-type drainage boards are arranged in a square pattern with a spacing of 0.9 meters and an average depth of 13.0 meters; horizontal drainage filter pipes and sealing devices are installed; a vacuum pumping device is set up for vacuum preloading. Vacuum preloading of the M-A5 area commenced on April 27, 2019, with the vacuum level quickly reaching 80 kPa and remaining stable. Stacking began on May 5, 2019, using mountain stone as the material, with a bulk weight of 17.5 kN/m^3 and a total stacking load of 4 meters. The stacking process lasted 20 days. On May 25, 2019, the project entered the vacuum joint preloading phase, concluding on August 23, 2019, totaling 119 days.

The monitoring points within the M-A5 zone are illustrated in Figure 1. This site boasts a comprehensive setup of 9 vacuum degree observers and an equal number of surface settlement gauges. Centrally positioned, a collection of layered sedimentation

tubes stands tall, each equipped with four inductive magnetic coils at depths of 3, 6, 9, and 12 meters, respectively. Correspondingly, pore water pressure transducers are interred at these precise levels. For the reinforcement project's security, an inclinometer casing reaching 7.5 meters deep and a water table monitoring pipe descending to 7 meters encircle the M-A5 region.

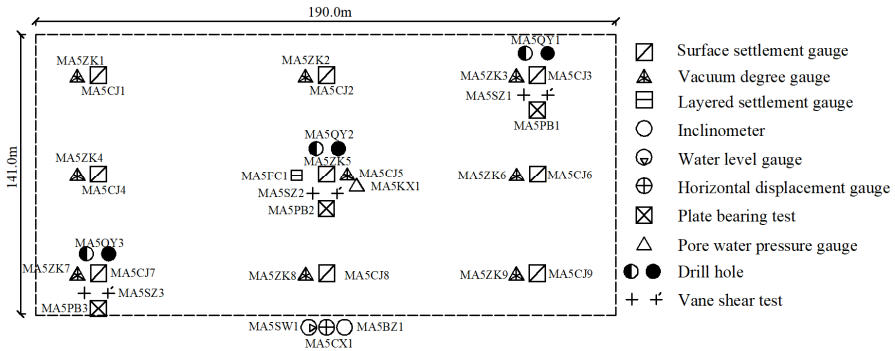


Fig. 1. M-A5 Regional monitoring point layout

2.2 Geological Conditions and Soil Properties

Based on the current drilling data, the M-A5 area encompasses three distinct engineering geological layers within its investigative depth: the initial layer primarily consists of fine sand and silt, while the third is characterized by silty clay. The ninth layer features argillaceous siltstone. A representative geological profile can be found in Figure 2. Within the reinforcement zone, the soft soil stratum comprises fine sand, compacted silt, and silty clay, exhibiting typical traits of weak soil with subpar engineering qualities. The key physical and mechanical properties of these soil layers are summarized in Table 1.

Table 1. Main physical property indexes of soil layer

Number	Layer	Thick-ness m	w %	p (g/cm ³)	e	G _s	E MPa	k _h (cm/s)	αMPa ⁻¹
①5-1	Blowfill silt	0~8.5	67	1.61	1.852	2.75	2.2	1.65	1.31
③7	Mucky clay	1.9~7.2	44.2	1.77	1.24	2.75	5.4	3.3	0.76

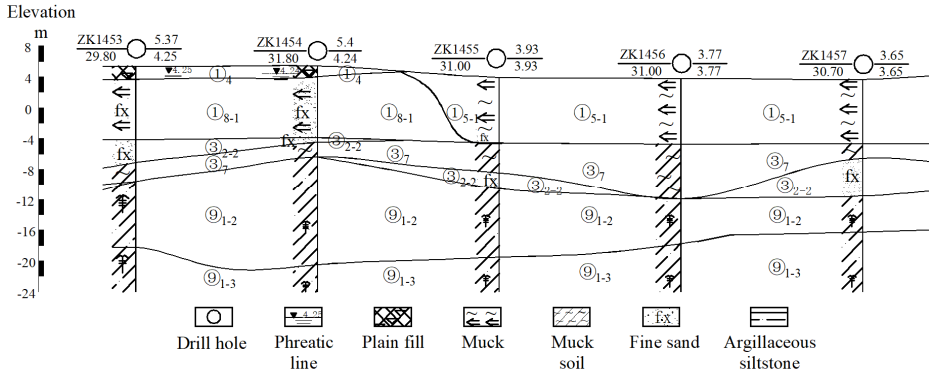


Fig. 2. Typical geological profile

3 Analysis of Monitoring Results of Vacuum Combined Preloading Method

3.1 Analysis of Variation Law of Surface Settlement

Figure 3 is the load-practice-settlement curve of each point in M-A5 region. In the figure, the vacuum load has been maintained in a relatively stable state and only changed greatly from August 1 to August 5 due to the influence of the typhoon. As can be seen from Figure 3, during the reinforcement of M-A5 region, the subsidence of the central region (MA5CJ2, MA5CJ5, MA5CJ8) and the eastern region (MA5CJ3, MA5CJ6, MA5CJ9) is greater than that of the western region (MA5CJ1, MA5CJ4, MA5CJ7), and their average subsidence amounts are 535.1mm respectively. 500.5mm, 318.4mm. This is not consistent with the shape of the foundation with the height on both sides and the middle low similar to the bottom of the pot formed by vacuum precompression method or vacuum combined load precompression method. The main reason for the settlement difference can be found by analyzing the geological profile; that is, the thickness of the fine powder layer in the west area where the settlement points MA5CJ1, MA5CJ4, and MA5CJ7 are located is larger than that in the middle and east areas. The lack of shallow silt layer, although the vacuum degree in the fine sand propagation loss is smaller, but the silt layer after treatment has a greater settlement, resulting in a small settlement on the west side. This shows that when the vacuum preloading method or vacuum combined preloading method is used to treat foundation-predicted settlement, the underlying soil layer should be analyzed first.

Table 2 Surface settlement rate of each stage of vacuum combined pile preloading. It can be found that in the early stage of vacuum pumping, the average settlement rate reaches 18.2 mm/d, which is much higher than that in the subsequent stage. This is because the shallow silt layer of the foundation as a whole is in a fluid plastic state under natural conditions, and the vacuum load causes the shallow soil to consolidate rapidly. An average settlement of 163.8 mm was produced over a short period of time.

The decrease in the settlement rate indicates that the foundation is constantly strengthening. The settlement rate in the loading stage is less than the stable vacuum rate, which can be explained from two aspects. First, the foundation as a whole has produced 241.5mm settlement at the end of the stable vacuum stage, reaching 53.3% of the final reinforcement settlement, indicating that the overall properties of the foundation have been improved; second, the settlement caused by the load has a hysteresis: from the perspective of effective stress, it takes time to discharge pore water due to the conversion of the load into the effective stress to cause settlement; from the vacuum load and the positive load mode of the load, it can be seen that the vacuum load causes horizontal inward displacement when the foundation is settled, and the positive load of the load produces horizontal displacement outward. The opposite horizontal displacement will also have a certain hindering effect on the vertical settlement of the load, causing the overall settlement rate of the foundation to decrease.

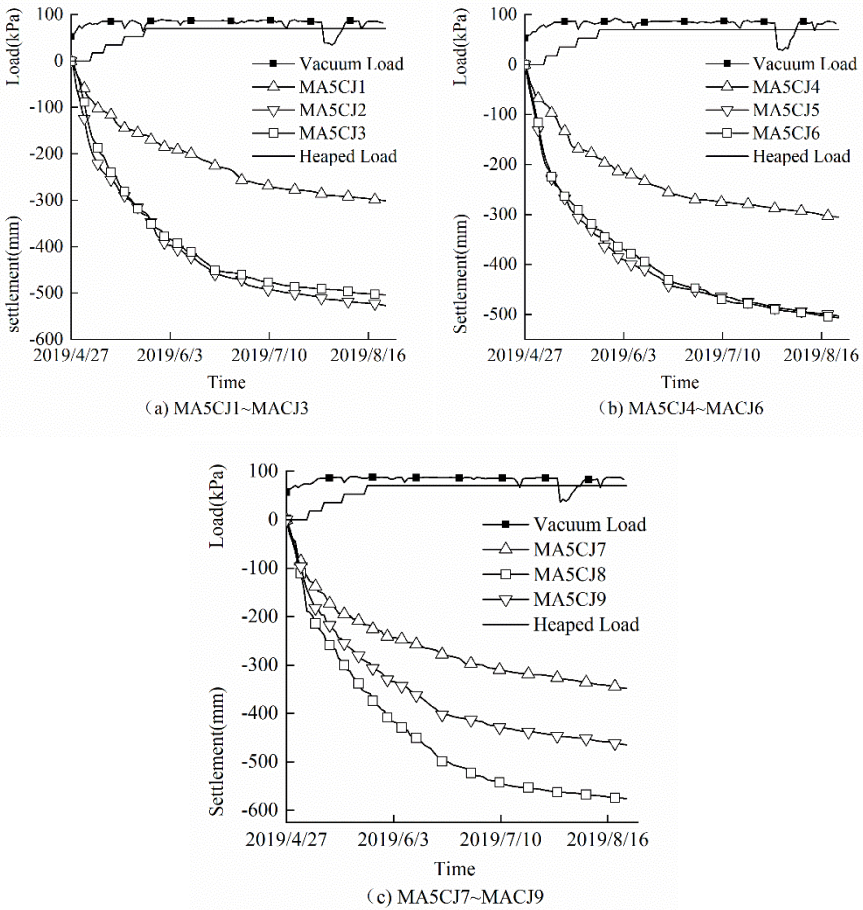


Fig. 3. Load-time-settlement

The hyperbolic method^[3] is used to calculate that the final settlement amount in the center of the reinforcement area is $S_{\infty}=565$ mm. The MA5CJ5 settlement amount is 503 mm, and the consolidation degree can be calculated as 89%, which meets the actual consolidation degree in the reinforcement project with no less than 85%, indicating that the vacuum combined load pre-pressure reinforcement effect is significant.

Table 2. Statistical table of surface settlement in each stage of solid area

Item	Vacuum- ing stage (9d)	Vacuum stabili- zation stage (10d)	Stowage phase (8d)	Combined pre- loading stage 90d	Average settling rate
$V(\text{mm}\cdot\text{d}^{-1})$	18.2	7.8	5.0	1.9	3.8
$V_{\max}(\text{mm}\cdot\text{d}^{-1})$	23.5	9.8	8.0	2.5	4.8
$V_{\min}(\text{mm}\cdot\text{d}^{-1})$	9.2	4.8	2.1	1.3	2.5
$S_{\text{ave}}(\text{mm})$	163.8	241.5	281.3	452.3	-

3.2 Analysis of Soil Layer Settlement Monitoring Results

Figure 4 is a layered settlement diagram at the center of the reinforcement zone. Comparing Figure 4, it can be found that the settlement of soil layer 0~6m is 374mm, accounting for 71.1% of the total settlement, and the settlement of soil layer below 6m accounts for 29.9%, indicating that the main area treated by vacuum combined loading preloading method is also shallow soil layer. Comparing the curves in the figure, it was found that the 6-9m settlement amount was 55mm, which was less than 9-12m settlement amount. Theoretically, the vacuum degree gradually decreases along the depth, and the lower soil layer should be smaller. Through the formation revealed by ZK1455 near the buried point of the layered settlement instrument, it can be found that the 6-9m blown silt layer is sandwiched with a 1.3m thick blown powder fine sand, while 9-12m is silt clay, which further shows that the silt soil layer of the same depth will produce a larger settlement.

3.3 Analysis of Pore Water Pressure and Groundwater Level

During the vacuum joint loading pre-pressure reinforcement process, changes in pore water pressure not only reflect the foundation consolidation but also highlight the unique characteristics of the vacuum joint loading pre-pressure method. Figures 5 and 6 illustrate the monitoring data for pore water pressure and groundwater level changes at various depths. Generally, pore pressure at all depths stabilizes over time and gradually converges, indicating that the consolidation process continues progressively. Initially, hole pressure exhibits significant fluctuations before stabilizing in the later stages. For instance, consider the hole pressure curves at -3m and -6m: the vacuum load rapidly decreases the hole pressure at these depths to negative values within a short period. Once the vacuum degree stabilizes, phased loading and groundwater level changes cause the hole pressure to display zigzag-like variations. Upon entering the joint reinforcement stage, as the groundwater level continues to decline and ultra-static

pore water pressure dissipates, the hole pressure at both depths continues to decrease and eventually stabilizes.

Judging from the reinforcement characteristics of the vacuum joint load pre-pressure method, both vacuum and load influence pore water pressure. The pore pressure at -6m decreases from 61kPa before reinforcement to -52kPa, resulting in a change amplitude of -113kPa. According to the negative pressure theory, the maximum vacuum load can only achieve -80kPa (below the membrane), causing the groundwater level to drop by 2.3m. The reduction in vacuum degree along the depth and the ultra-static pore water pressure due to positive load cannot be fully explained. However, this phenomenon can be understood using the effective stress growth method. Firstly, the load and vacuum load are treated as two independent processes. For the load, the generated ultra-static pore water pressure is positive and gradually dissipates with consolidation; meanwhile, the vacuum load reduces the pore water pressure to a negative value, stabilizing and converging with consolidation. From an effective stress perspective, these processes combine to reinforce the soil. Initially, the vacuum load rapidly reduces pore water pressure and increases effective stress, aligning with formula (2). During the loading stage, the applied load generates ultra-static pore water pressure, causing a sudden increase that dissipates over time, thereby increasing effective stress, corresponding to formula (1) and serrated changes in pore water pressure. After partial dissipation of the ultra-static pore water pressure from the stack load, effective stress continues to increase. For formula (2), the effective stress also rises, necessitating an increase in negative pore water pressure to maintain equilibrium. Consequently, when the vacuum load drops the pore pressure at 6m and stabilizes it, the pore water pressure continues to decline, ultimately changing by -113kPa.

$$\Delta\sigma = \Delta\sigma' + \Delta u \tag{1}$$

$$0 = \Delta\sigma' + \Delta u \tag{2}$$

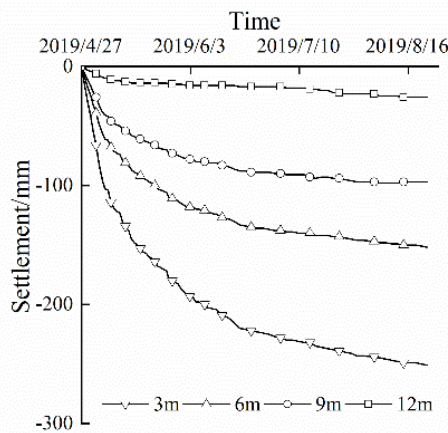


Fig. 4. Stratified settlement Figure

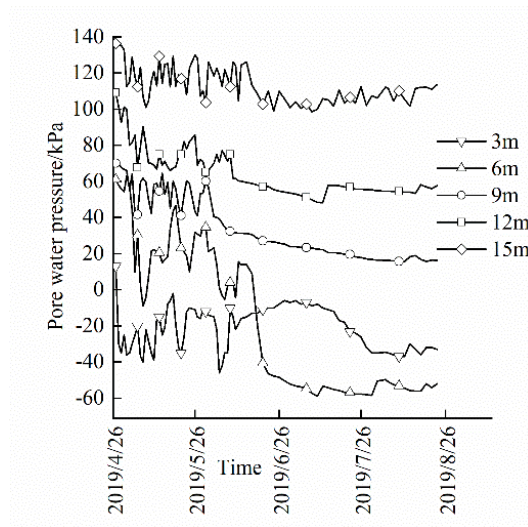


Fig. 5. Pore water pressure monitoring curve

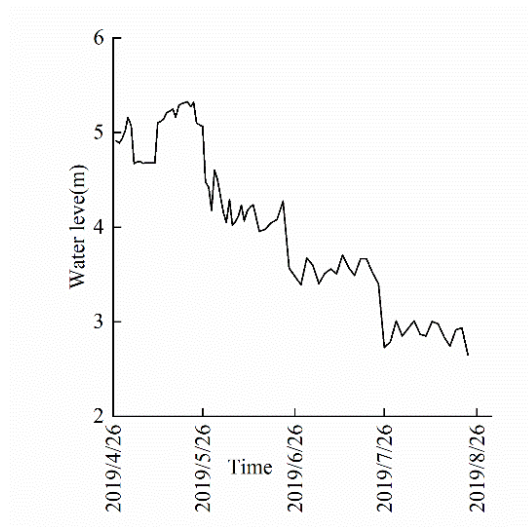


Fig. 6. Groundwater level change curve

But evidently, the ultrastatic pore water pressure engendered by the loading has not been entirely dissipated [1]. This can be discerned by juxtaposing the pore pressure curves at 3m and 6m. With the diminution in the vacuum degree during the downward transmission process, the negative pressure value at 3m ought to be lesser than that at 6m. However, the distribution of additional stress along the depth due to the loading effect varies, resulting in the negative pressure value at 3m being greater than that at 6m under the influence of ultrastatic pore water pressure.

From the aforementioned analysis, it can be deduced that the change in pore pressure during the reinforcement process of vacuum combined load pre-preSSION is intricate, particularly when the ratio of the stack load and vacuum load approximates 1:1 (when the ratio of the two is less than 1:2, the pore pressure curve mirrors the alteration in the pore pressure curve in the vacuum pre-preSSION method). The complex fluctuations in pore pressure unveil the diversity of effective stress growth during the reinforcement process and the challenge in ascertaining the degree of foundation consolidation. Consequently, the current methodology for calculating vacuum combined load pre-load consolidation of vacuum joint loads, which is widely analogous to stack loads, necessitates refinement.

3.4 Analysis of Soil Horizontal Displacement Change Law

The inclined tube MA5CX1 monitors the deep horizontal displacement in the M-A5 area, as illustrated in Figure 7. A positive value indicates a reduction in horizontal displacement towards the reinforcement zone. The figure reveals that the foundation soil contracts horizontally inward overall, with the maximum displacement of 49mm occurring at the surface. As the reinforcement progresses, the soil at a depth of 7m shows minor horizontal displacement outside the reinforcement area. This suggests that the horizontal displacement during reinforcement is minimal, eliminating concerns about shear failure due to stacking, and indicating successful overall reinforcement.

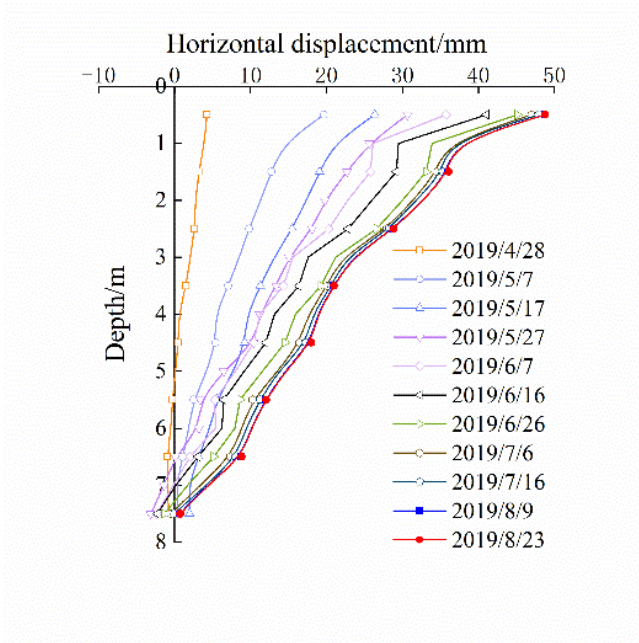


Fig. 7. Horizontal displacement - time curve

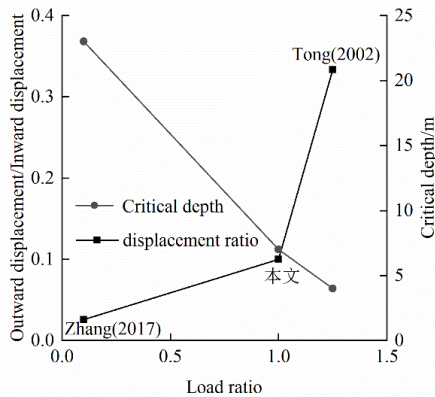


Fig. 8. Displacement ratio - load ratio - critical depth curve

Based on previous scholars' research, we found that^[2, 4]: The development of horizontal displacement in vacuum combined load precompression method is mainly related to the load ratio of vacuum load and load, and the development of horizontal displacement is mainly measured by the displacement ratio (displacement outside the reinforcement area/displacement inside the reinforcement area) and critical depth (deep of outward displacement in the reinforcement area). According to the analysis of Figure 8, it can be found that the load ratio significantly affects the development of horizontal displacement. When the load ratio is less than 1:1, the load can hardly cause the outward horizontal displacement of the soil, which is generally less than 1/10 of vertical settlement, or the displacement is smaller as shown in the figure, and in this case the load ratio is close to 1:1; when the load ratio is greater than 1:1, a significant outward horizontal displacement will occur in the soil, even reaching 1/3 of the inward horizontal displacement. At this time, the critical points of horizontal inward displacement and outward displacement are higher than other cases, which are determined by additional lateral stress caused by the two loads. When the critical depth is higher, the thickness of the soil layer corresponding to the outward horizontal displacement in the soil body will be greater.

4 Conclusion

(1) The significant settlement disparity within the reinforcement zone primarily stems from fluctuations in the thickness of the sludge layer beneath the cover soil. Notably, during the vacuum phase, the apex settlement rate reaches 18.2mm/d, a figure substantially higher than that observed throughout the consolidated reinforcement stages, thereby illustrating a delayed response to loading effects. Employing the hyperbolic model, the ultimate settlement at the foundation's core was estimated at 565mm, with the ground consolidation level attaining an impressive 89%, affirming the efficacy of the overall reinforcement strategy.

(2) Remarkably, settlement occurring between the surface and a depth of 6 meters constitutes a dominant 71.1% of the total settlement experienced, underscoring the critical importance of this particular stratum in settlement analysis.

(3) From an effective stress standpoint, the post-loading dissipation of excess pore pressure significantly influences the vacuum-induced negative pressures, leading to a notable shift in pore pressure at the 6-meter mark to -113kPa. This value surpasses the maximum achievable vacuum degree, highlighting the intricate interplay between pore pressure dynamics and vacuum loading mechanisms.

(4) In vacuum joint loading pre-pressure reinforcement foundation engineering, the horizontal displacement ratio of the center of the reinforcement area is related to the load ratio. The larger the load ratio, the larger the displacement ratio, and the shallower the critical depth.

This paper mainly analyzes the monitoring data of blown-fill foundation treated by vacuum combined loading pre-pressure method, and obtains the mechanism of vacuum combined loading pre-pressure method and the characteristics of soil layer change. The follow-up research can be combined with laboratory tests to analyze the microscopic properties of blown-fill soil and further analyze the reinforcement mechanism of soil layer under vacuum combined loading pre-pressure.

Acknowledgments

The completion of this work was supported by Collaborative Innovation Center for Natural Resources Planning and Marine Technology of Guangzhou (No.2023B04J0301, 2025B04J0030). The Science and Technology Foundation of Guangzhou Urban Planning and Design Survey Research Institute (Grant No. RDI2230204030), Last but not least, many thanks for the support of Academic Specialty Group for Urban Sensing in Chinese Society of Urban Planning.

References

1. KJELLMAN W. Consolidation of clay by heart of atmosphere pressure//Proceedings of the Conference on Soil Stabilization. Boston: Massachusetts Institute of Technology, 1952: 258-263.
2. Holtz R D, Wager O. Preloading by vacuum: current prospects. Transportation research record, 1975548:26-29.
3. Holtan G W. Vacuum stabilization of subsoil beneath runway extension at Philadelphia International Airport//Proc. of 6th ICSMFE. 1965
4. Johnson S J. State-of-the-Art applicability of conventional densification techniques to increase disposal area storage capacity. US Waterways Experiment Station, 1977.
5. Hammer D P. Evaluation of Underdrainage Techniques for the Densification of Fine-Grained Dredged Material. ARMY ENGINEER WATERWAYS EXPERIMENT STATION VICKSBURG MENVIRONMENTAL LAB.1981.

6. Sandiford R E, Ludewig N, Dunlop P. Evaluation of enhanced consolidation for dredged material disposal Newark bay confined disposal facility//International Workshop on Technology Transfer for Vacuum-induced Consolidation: Engineering and Practice, Los Angeles, California. 1996: 31-37.
7. S. Sivaraman, Kasinathan Muthukkumaran. Non-linear performance analysis of free headed piles in consolidating soil subjected to lateral loads. *Engineering Science and Technology, an International Journal*,2021,Vol.24(2): 449-457.
8. Ding-Bao Song,Kai Lou,Wen-Bo ChenCA1,et al. Finite strain elastic visco-plastic consolidation model for layered soils with vertical drain considering self-weight loading and non-linear creep. *Computers and Geotechnics*,2024,Vol.169: 106180.
9. Sun, L.-Q.,Yan,et al. Finite element analysis of reclaimed soil foundation consolidated by surcharge preloading combined with vacuum preloading(Article). *Yantu Gongcheng Xuebao/Chinese Journal of Geotechnical Engineering*,2010,Vol.32(4): 592-599.
10. Lei Zhang,Haihui Jin,Yandong Lv,et al. Improvements in vacuum-surcharge preloading combined with electro-osmotic consolidation on soft clayey soil with high water content. *Geotextiles and Geomembranes*,2025,Vol.53(1): 41-54.
11. Baral P, Rujikiatkamjorn C, Indraratna B, Kelly R. Radial consolidation characteristics of soft undisturbed clay based on large specimens. *Journal of Rock Mechanics and Geotechnical Engineering* 2018;10(6):1037e45.
12. Chai JC, Carter JP, Hayashi S. Ground deformation induced by vacuum consolidation. *Journal of Geotechnical and Geoenvironmental Engineering* 2005;131(12):1552e61.
13. Chu J, Yan SW, Yang H. Soil improvement by the vacuum preloading method for an oil storage station. *Geotechnique* 2000;50(6):625e32.
14. Indraratna B, Balasubramaniam AS, Sivaneswaran N. Analysis of settlements and lateral deformation of soft clay foundation beneath two embankments. *Inter-national Journal of Numerical and Analytical Methods in Geomechanics*1997;31(9):599e618.
15. Indraratna B, Redana IW. Numerical modeling of vertical drains with smear and well resistance installed in soft clay. *Canadian Geotechnical Journal* 2000;37(1):132e45

Open Access This chapter is licensed under the terms of the Creative Commons Attribution-NonCommercial 4.0 International License (<http://creativecommons.org/licenses/by-nc/4.0/>), which permits any noncommercial use, sharing, adaptation, distribution and reproduction in any medium or format, as long as you give appropriate credit to the original author(s) and the source, provide a link to the Creative Commons license and indicate if changes were made.

The images or other third party material in this chapter are included in the chapter's Creative Commons license, unless indicated otherwise in a credit line to the material. If material is not included in the chapter's Creative Commons license and your intended use is not permitted by statutory regulation or exceeds the permitted use, you will need to obtain permission directly from the copyright holder.

